

Coherent control of double-dot molecules using Aharonov-Bohm magnetic fluxMatisse Wei-Yuan Tu,^{1,2} Wei-Min Zhang,^{1,2,*} and Franco Nori^{2,3,†}¹*Department of Physics, National Cheng Kung University, Tainan 70101, Taiwan*²*Advanced Science Institute, RIKEN, Saitama 351-0198, Japan*³*Physics Department, The University of Michigan, Ann Arbor, Michigan 48109-1040, USA*

(Received 14 May 2012; revised manuscript received 17 October 2012; published 2 November 2012)

Bonding and antibonding states of artificial molecules have been realized in experiments by directly coupling two quantum dots. Without a direct coupling between two nearby quantum dots, here we show that under a very unusual condition (i.e., a large asymmetrical couplings to the leads at a large bias) continuous coherence control of double-dot charge states can be achieved by changing the flux through a double-quantum-dot Aharonov-Bohm (AB) interferometer. Using magnetic flux to control double-dot molecular-state coherence is very robust against charge noise. We explicitly present the flux-dependent real-time processes of molecular-state formation. In contrast with the transport current, which has a 2π period, the quantum state of the double-quantum-dot molecule has a 4π period in the AB flux.

DOI: 10.1103/PhysRevB.86.195403

PACS number(s): 73.63.Kv, 03.65.Wj

I. INTRODUCTION

It is important to tailor quantum states, especially, to control the coherent phase between two superposition states. In the past decades, artificial atoms and molecules in solid-state systems, such as superconducting Josephson junctions¹ and semiconductor quantum dots (QDs)^{2–4} have provided novel platforms for exploring such quantum-coherent effects. Due to the tunability of various electronic couplings, double-quantum-dot (DQD) systems, which are archetypes of artificial molecules, have attracted considerable attention because they can serve as qubit systems for quantum information processing.^{5,6} The two DQD charge states with one electron residing in either of the two dots are defined as the computational basis of the DQD charge qubit. Coherence arising from superpositions between such charge qubit states, called DQD molecular states in this paper, is of primary interest. It can be achieved by directly coupling the two quantum dots. The tunability of such direct interdot coupling has been experimentally demonstrated^{7,8} and the charge coherence has also been observed in various experiments.^{3,4,9–12} However, the tunnel coupling between the charge states is implemented via voltage gates, which is susceptible to charge noises.^{13–15}

In this paper, we show that for a uncoupled DQD in an Aharonov-Bohm (AB) interferometer, by solely tuning the AB flux, the coherent control of the DQD charge states can be realized. Controlling the charge coherence via magnetic fields could circumvent charge noise. Magnetic fluxes have been utilized to investigate the coherence of electron transport through a single QD in AB interferometers.¹⁶ Combining an interdot tunnel coupling with a magnetic flux has also been studied theoretically^{17–19} and experimentally.^{20–23} In particular, controlling the DQD molecular states through AB phases has been of recent experimental interest.²⁰ Besides the charge noise induced from voltage gates, coupling the DQD to electrodes also causes decoherence.^{24–26} Although the tunnelings to the electrodes may be turned off to avoid the electron-reservoirs-induced decoherence, such tunnelings are indispensable for the AB effect. Thus, controlling the charge coherence of the uncoupled DQD through the AB flux is very robust against charge noises but it still faces the challenge of the electron-reservoir-induced decoherence.

In this paper, we consider an uncoupled DQD embedded in an AB interferometer, as shown in Fig. 1. In contrast to previous theoretical studies, which focused on quantum transport,^{27–32} here we directly exploit the quantum coherence between the charge qubit states in this DQD molecule. Usually charge coherence control is performed with symmetric couplings to leads via electric gate fields. However, for the quantum dot Aharonov-Bohm interferometer, the symmetrical coupling causes the phase localization as we have shown in the recent publication,³³ which hinders the coherence control in the usual way. We find that under a very unusual condition, namely using a large asymmetric coupling to the leads, in strong contrast to the usual condition of the coherent control with symmetric couplings, one is able to control charge coherence via magnetic flux at a large bias. By analyzing the detailed decoherence through the AB flux, the time-resolved formation processes of various molecular states with different AB fluxes are explicitly presented. Furthermore, we find that the period of the DQD molecular states is 4π in the AB flux. Instead, the transport current, obtained by averaging the DQD states, has a period of 2π . The coherence of the DQD molecular states and the coherence of electron transport flowing through the DQD therefore manifest themselves fundamentally different with respect to the AB flux.

The paper is organized as follows. In Sec. II, we describe the double-dot AB interferometer and solve exactly the reduced density matrix of the double dot. In Sec. III, we explore the coherence controls of the DQD molecular states via the AB flux. In Sec. IV, the real-time processes of the DQD molecular state formations are presented in different pictures. And the discussion and conclusion are given in Sec. V.

II. MODEL SYSTEM AND ITS EXACT SOLUTION

To focus on the influence of the AB flux on the quantum state of the artificial molecule we consider only polarized noninteracting electrons. The total Hamiltonian of the system is conventionally²⁸ given by $\mathcal{H} = \mathcal{H}_s + \mathcal{H}_E + \mathcal{H}_T$, in which $\mathcal{H}_s = \sum_i E_i a_i^\dagger a_i$ describes an uncoupled DQD and $\mathcal{H}_E = \sum_{\alpha k} \epsilon_{\alpha k} c_{\alpha k}^\dagger c_{\alpha k}$ is the Hamiltonian for the leads with $\alpha = L(R)$

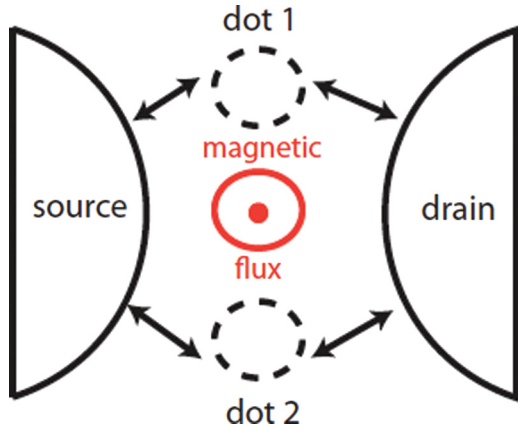


FIG. 1. (Color online) Schematic diagram of a pair of uncoupled quantum dots in an Aharonov-Bohm interferometer.

labeling the source (drain) lead, and $\mathcal{H}_T = \sum_{j\alpha k} [V_{j\alpha} c_{\alpha k}^\dagger a_j + \text{H.c.}]$ depicts the coupling between the central dot system and the leads. Here a_i^\dagger (a_i) and $c_{\alpha k}^\dagger$ ($c_{\alpha k}$) are the electron creation (annihilation) operators for the electronic levels i and k in the dot system and the lead α , respectively. The tunneling amplitudes harbor the applied magnetic flux Φ via $V_{jL} = \bar{V}_{jL} e^{-i\phi_{jL}}$ and $V_{jR} = \bar{V}_{jR} e^{i\phi_{jR}}$ with the relation $\phi_{1L} - \phi_{2L} + \phi_{1R} - \phi_{2R} = \phi \equiv 2\pi\Phi/\Phi_0$, where $\phi = 2\pi\Phi/\Phi_0$ and $\Phi_0 = h/e$ is the flux quantum. The line widths induced by tunneling are then given by $\Gamma_\alpha = 2\pi|V_{j\alpha}|^2 \rho_\alpha$, where ρ_α is the density of states in the lead α . The DQD molecular states described in terms of the reduced density matrix are governed by the following exact master equation:²⁶

$$\frac{d}{dt}\rho(t) = -i[\mathcal{H}_s, \rho(t)] + \sum_{i\alpha} [\mathcal{L}_{i\alpha}^+(t) + \mathcal{L}_{i\alpha}^-(t)]\rho(t), \quad (1)$$

where $\mathcal{L}_{i\alpha}^\pm(t)$ are the superoperators describing the dissipations and fluctuations induced by the tunnel coupling to the electrodes (for details see Ref. 26). Denoting the state of the empty DQD by $|0\rangle$, one electron on the first and the second dots by $|1\rangle$ and $|2\rangle$, respectively, and the state of both dots occupied by $|3\rangle$, the density matrix $\rho(t)$ can be generally expressed as

$$\rho(t) = \begin{pmatrix} \rho_{00}(t) & 0 & 0 & 0 \\ 0 & \rho_{11}(t) & \rho_{12}(t) & 0 \\ 0 & \rho_{21}(t) & \rho_{22}(t) & 0 \\ 0 & 0 & 0 & \rho_{33}(t) \end{pmatrix}, \quad (2)$$

where $\rho_{ij} = \langle i|\rho|j\rangle$ with $i, j = 0, 1, 2, 3$. The QDQ molecular state, featured as one electron in the DQD shared between the two charge states of the DQD molecule, is embedded in the central 2×2 block matrix of Eq. (2).

To see how molecular states in this DQD are formed in time, we solve the master equation (1) with the initial preparation of the empty DQD, namely, $\rho_{00}(0) = 1$ and $\rho_{ij}(0) = 0$, for all $i \neq 0, j \neq 0$. The exact solution from the master equation for each matrix element gives

$$\begin{aligned} \rho_{11}(t) &= v_{11}(t) - \det \mathbf{v}(t), \\ \rho_{22}(t) &= v_{22}(t) - \det \mathbf{v}(t), \\ \rho_{12}(t) &= v_{12}(t), \quad \rho_{21}(t) = v_{21}(t), \\ \rho_{00}(t) &= \det[I - \mathbf{v}(t)], \quad \rho_{33}(t) = \det \mathbf{v}(t), \end{aligned} \quad (3)$$

with I being an identity matrix and

$$\mathbf{v}(t) = \int \frac{d\omega}{2\pi} \mathbf{u}(t, \omega) \sum_{\alpha} f_{\alpha}(\omega) \Gamma_{\alpha} \begin{pmatrix} 1 & e^{\pm i\phi/2} \\ e^{\mp i\phi/2} & 1 \end{pmatrix} \mathbf{u}^{\dagger}(t, \omega) \quad (4)$$

is a 2×2 hermitian matrix, where $f_{\alpha}(\omega)$ is the Fermi distribution function of the reservoirs, the upper (lower) sign is for $\alpha = L$ (R), and $\mathbf{u}(t, \omega) = \int_{t_0}^t d\tau e^{i\omega(t-\tau)} \mathbf{u}(\tau)$ with

$$\mathbf{u}(\tau) = \exp \left[- \begin{pmatrix} iE_1 + \Gamma & \Gamma_c(\phi) \\ \Gamma_c^*(\phi) & iE_2 + \Gamma \end{pmatrix} \tau \right]. \quad (5)$$

Here we have defined $\Gamma_c(\phi) = \Gamma \cos(\phi/2) + i\delta\Gamma \sin(\phi/2)$ with $\Gamma = \Gamma_L + \Gamma_R$ and $\delta\Gamma = \Gamma_L - \Gamma_R$. The functions $\mathbf{u}(t)$ and $\mathbf{v}(t)$ are indeed the spectral and correlation Green functions in the Schwinger-Keldysh nonequilibrium Green function theory.³⁴ The AB flux ϕ , the coupling asymmetry $\delta\Gamma$, the non-degeneracy $\delta E = E_1 - E_2$, and the nonequilibrium dynamics from the electron tunnelings all influence the consequent quantum states of the DQD molecule.

On the other hand, we can rewrite the DQD molecular state [i.e., the central block matrix of Eq. (2)] as

$$\rho_q(t) = \frac{1}{2}[I + \mathbf{r}(t) \cdot \boldsymbol{\sigma}] - \frac{1}{2}[\rho_{00}(t) + \rho_{33}(t)]I, \quad (6)$$

where $\boldsymbol{\sigma} = (\sigma_x, \sigma_y, \sigma_z)$ consists of the Pauli matrices and $\mathbf{r}(t) = (r_x, r_y, r_z)$ with

$$r_x = 2\text{Re}\rho_{21}(t), \quad r_y = 2\text{Im}\rho_{21}(t), \quad r_z = 2[\rho_{11}(t) - \rho_{22}(t)], \quad (7)$$

being the polarization vector for the molecular states. So the coherence dynamics of DQD molecular state formations, described by the off-diagonal matrix element ρ_{12} of the reduced density matrix, can also be visualized through the motion of the polarization vector with the Bloch sphere. Also, the leakage out of the one-electron state space can be easily seen from the term proportional to the probability of the empty and the doubly occupied states, $\rho_{00}(t) + \rho_{33}(t)$.

III. COHERENT PHASES CONTROLLED BY THE AB FLUX

The coherence between the two charge states of the DQD molecule is characterized by the off-diagonal element ρ_{21} . To develop a clear picture of the coherence of the DQD molecular state, let us first look at the off-diagonal matrix element $\rho_{12}(t)$ in Eq. (3) in the steady-state limit ($t \gg \Gamma^{-1}$) at zero temperature. The general solution is

$$\begin{aligned} \rho_{21} &= \frac{1}{2}(r_x + ir_y) \\ &= \frac{1}{2\pi} \left[\tan^{-1} \left(\frac{eV}{2\Gamma_+(\phi)} \right) + \tan^{-1} \left(\frac{eV}{2\Gamma_-(\phi)} \right) \right] \\ &\quad \times \left[\frac{\delta\Gamma}{\Gamma} \cos \frac{\phi}{2} - i \sin \frac{\phi}{2} \right] + \frac{\delta E}{4\pi\gamma(\phi)} \left[\frac{1}{\Gamma_+(\phi)} \right. \\ &\quad \times \tan^{-1} \left(\frac{eV}{2\Gamma_+(\phi)} \right) - \frac{1}{\Gamma_-(\phi)} \tan^{-1} \left(\frac{eV}{2\Gamma_-(\phi)} \right) \left. \right] \\ &\quad \times \left\{ \frac{1}{\Gamma} \left[(\Gamma^2 - \delta\Gamma^2) \sin \frac{\phi}{2} - \delta\Gamma\delta E \cos \frac{\phi}{2} \right] - i\delta E \sin \frac{\phi}{2} \right\}, \end{aligned} \quad (8)$$

where $\gamma(\phi) = \sqrt{\Gamma^2 \cos^2(\phi/2) + \delta\Gamma^2 \sin^2(\phi/2) - \delta E^2}$ and $\Gamma_{\pm}(\phi) = 2^{-1}[\Gamma \pm \gamma(\phi)]$. Here, we have also applied a bias, $\mu_L = eV/2 = -\mu_R$. The full complexity of decoherence is revealed through Eq. (8). Due to severe decoherence in such a system, it has been analytically proven³³ and also numerically demonstrated later³⁵ that the coherent phase φ (in the off-diagonal matrix element $\rho_{21} = |\rho_{21}|e^{i\varphi}$) between the two DQD charge qubit states can only take the values of 0, $\pm\pi/2$ or π for arbitrary flux. This applies for the often-used condition of degeneracy $\delta E = 0$ and symmetric coupling $\delta\Gamma = 0$. Such decoherence-induced localization of the coherent phase hinders the manipulation of the coherent phase of molecular states. Remarkably, when the DQD couples largely asymmetrical to the left and the right leads ($\delta\Gamma \neq 0$), we find that the coherent phase φ can be continuously tuned by AB fluxes.

To achieve typical molecular states, the DQD is set at degeneracy ($\delta E = 0$). Then the second term in Eq. (8) vanishes. Equations (3) and (8) show that the formation of molecular states is essentially determined by the applied bias and the coupling asymmetry to the source and the drain. The basic setup of zero bias (which is commonly used for examining quantum transport) leads to $\rho_{21} = 0$ (where the DQD is in equilibration with the reservoirs) and is not of interest here. With a large bias $eV \gg \Gamma$, we find

$$\rho_{21} = \begin{cases} \frac{1}{2}[(\delta\Gamma/\Gamma) \cos \frac{\phi}{2} - i \sin \frac{\phi}{2}] & \text{if } \phi \neq 0, \\ \frac{1}{4}(1 + \delta\Gamma/\Gamma) & \text{if } \phi = 0. \end{cases} \quad (9)$$

Equation (9) clearly shows the controllability of the coherent phase between the two charge states of the DQD molecule through the AB flux. It also explicitly reveals the necessity of the asymmetry in the couplings $\delta\Gamma \neq 0$. In the case of symmetric coupling $\delta\Gamma = 0$, Eq. (9) shows that the real part vanishes for $\phi \neq 0$ so that the coherent phase φ is localized at $\pi/2$, except for $\phi = 0$, where the coherence phase is restricted to 0, as pointed out by the authors of Ref. 33. This result has recently been reproduced using the exact numerical path-integral method³⁵ where the e - e interaction was also included. However, with the larger asymmetry $\delta\Gamma$, the coherence amplitude $|\rho_{21}|$ linearly increases and the coherence phase is continually driven by the AB flux, as seen from Eq. (9).³⁶ By setting $\delta\Gamma \lesssim \Gamma$, we obtain $\rho \approx |\psi(\phi)\rangle\langle\psi(\phi)|$, where

$$|\psi(\phi)\rangle = \frac{1}{\sqrt{2}}[|1\rangle + \exp(-i\phi/2)|2\rangle]. \quad (10)$$

A continuous transition from the symmetric molecular state $|\psi(0)\rangle = (|1\rangle + |2\rangle)/\sqrt{2}$ to the antisymmetric molecular state $|\psi(\pm 2\pi)\rangle = (|1\rangle - |2\rangle)/\sqrt{2}$ is achieved by changing the AB flux, as shown in Fig. 2 (and the interpretation given in the figure caption). Interestingly, we also find that the period of the state of the DQD molecule is 4π , rather than the usual 2π in the AB flux.

The physics behind this coherence tunability is as follows. The coherence between the charge states $|1\rangle$ and $|2\rangle$ is related to the molecular basis $|\pm\rangle = \frac{1}{\sqrt{2}}(|1\rangle \pm |2\rangle)$ via $\text{Re}\rho_{21} = \frac{1}{2}(\rho_{+,+} - \rho_{-,-})$ and $\text{Im}\rho_{21} = \text{Im}\rho_{+,-}$. With a symmetric geometry of the system $\delta E = 0$ and $\delta\Gamma = 0$, neither of the molecular states $|\pm\rangle$ is preferred. This results in $\rho_{+,+} = \rho_{-,-}$

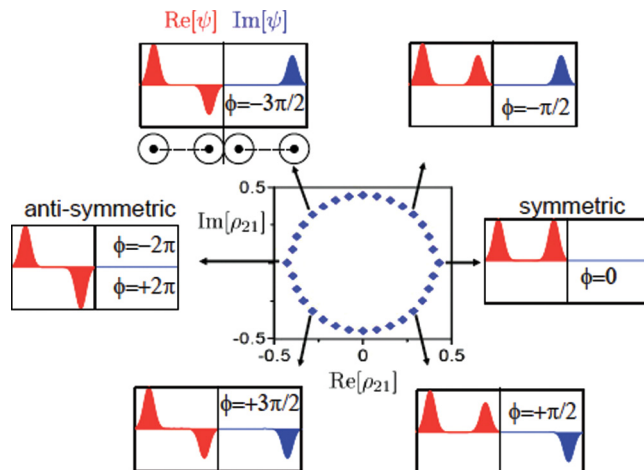


FIG. 2. (Color online) Control of the coherent phase of the DQD molecule by the AB flux. The explicit solution of ρ_{21} in the steady-state limit is shown by the “blue diamonds” on the central panel. Each diamond corresponds to an AB flux value, taken from $\phi = 0$ to $\phi = \pm 2\pi$ with $\pi/8$ steps. The wave functions on the DQD molecules are illustrated for various values of the AB flux. A DQD is indicated by two circles with centers connected by a dashed line (no interdot coupling) below the diagrams for $\phi = -3\pi/2$. Both the real (red) and the imaginary (blue) parts are shown, so one sees how the AB flux changes the coherent phase between the two charge states. Other parameters are $\delta E = 0$, $eV = 6\Gamma$ at $k_B T = \Gamma/20$, which are also used in the following figures, unless specified.

so that $\text{Re}\rho_{21} = 0$. Therefore the phase of ρ_{21} can only be $\pm\pi/2$ (i.e., the phase localization shown in previous work³³). In the case that $\phi = 0$ (or $\phi = 2\pi$), the state $|-\rangle$ (or $|+\rangle$) becomes decoupled from the electron reservoirs, and electrons can only occupy the opposite molecular state $|+\rangle$ (or $|-\rangle$). The corresponding phase of ρ_{21} is then 0 (or π). On the other hand, when $\phi = 0$, the occupation of the antisymmetric state $|-\rangle = (|1\rangle - |2\rangle)/\sqrt{2}$ becomes a constant of motion.³⁷ Turning on the flux $\phi \neq 0$ breaks such symmetry and consequently changes the electron states abruptly. Therefore ρ_{21} changes abruptly across $\phi = 0$ as indicated in Eq. (9).

IV. REAL-TIME PROCESSES OF MOLECULAR-STATE FORMATIONS

The full information of the quantum state of the DQD molecule at finite temperature is depicted by the time-dependent reduced density matrix. In Fig. 3, we plot the evolution of the full reduced density matrix of the DQD molecule. Initially, the DQD is prepared in an empty state, $\rho_{00}(0) = 1$ as shown by Figs. 3(b1), 3(c1), and 3(d1) and $\mathbf{r}(0) = 0$ given in Fig. 3(a1) (where the length of the red strip is zero). After injecting electrons from the left and the right reservoirs, ρ_{00} decreases [see Figs. 3(b1) to 3(b3)] while the electron occupation and coherence increase with time [see Figs. 3(b1) to 3(b3), Figs. 3(c1) to 3(c3), and also Figs. 3(d1) to 3(d3)]. The coherent phase φ between the charge states has been fixed shortly after the electron injection [see Figs. 3(a1) to 3(a4) and also Figs. 3(d2) to 3(d4)]. Then $|\mathbf{r}(t)|$ grows in time with fixed φ , and finally a stable molecular state, $\rho \approx |\psi\rangle\langle\psi|$, where $|\psi\rangle = (|1\rangle + e^{-i\phi/2}|2\rangle)/\sqrt{2}$, is reached in a short time,

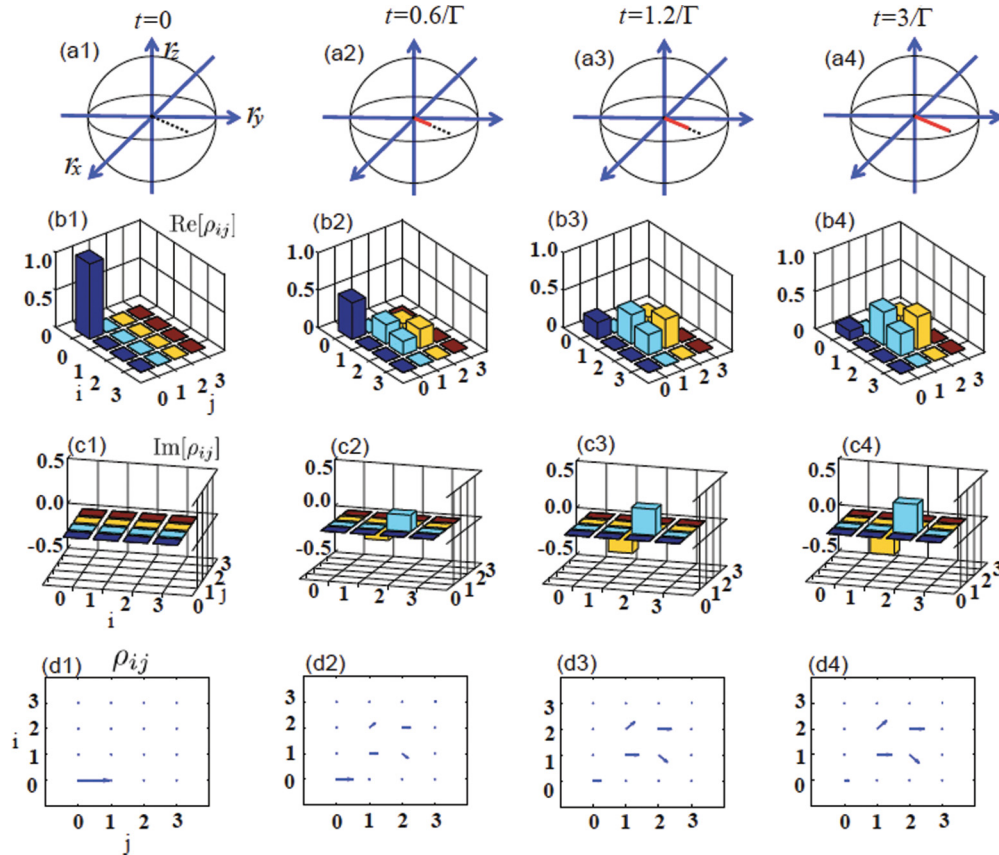


FIG. 3. (Color online) Typical process for forming molecular states. The dashed black line in (a1) to (a4) is the trajectory taken by $\mathbf{r}(t)$ from $t = 0$ in (a1), starting from the origin, to $t = 3/\Gamma$ in (a4), where it almost touches the surface of the sphere. The red strip in each plot is the trajectory up to the corresponding time points, as shown above the spheres. From the trajectory, we see the coherent phase φ [which is the angle made by $\mathbf{r}(t)$ with r_x axis] has been fixed after the electron is injected into the DQD. Plots (b1) to (b4) display the real part of the reduced density matrix of the DQD system, while the imaginary part is plotted in (c1) through (c4). The coherent phase φ between the two charge states is better visualized through the vector plots (d1) to (d4). Every arrow represents an element of the reduced density matrix ρ_{ij} , whose horizontal projection stands for the real part and the vertical projection stands for the imaginary part. The AB flux here is $\phi = -\pi/2$.

of about $3\Gamma^{-1}$. Note that due to possible leakage, see Fig. 3(b3) where ρ_{00} has a small finite value, the DQD is not in a perfect pure state. But the situation can be optimized by changing the bias and the coupling asymmetry, as shown by Eq. (9).

To better understand the role played by the AB flux, we show the time evolutions of ρ_{21} in Fig. 4 under various values of ϕ . Figures 4(a1) and 4(a2) show the process of coherence generation for a strong asymmetrical coupling (with $\delta\Gamma = 0.9\Gamma$). The rate of approaching steady-coherent-molecular states is only weakly dependent on the flux. The stable molecular states are soon reached after a few Γ^{-1} . This is totally different from the symmetrical coupling ($\delta\Gamma = 0$), as shown by the authors of Refs. 33 and 35, where $\text{Re}\rho_{21}$ displays the severe flux-dependent decays due to the decoherence induced by the large electron transport in the symmetrical coupling. Therefore, the larger coupling asymmetry can strongly suppress the decoherence from the electron transitions, and makes the coherence control of the QDQ molecule feasible.

V. DISCUSSIONS

The general solution shows that the quantum state of the DQD molecule has a period of 4π in the AB flux. It is an

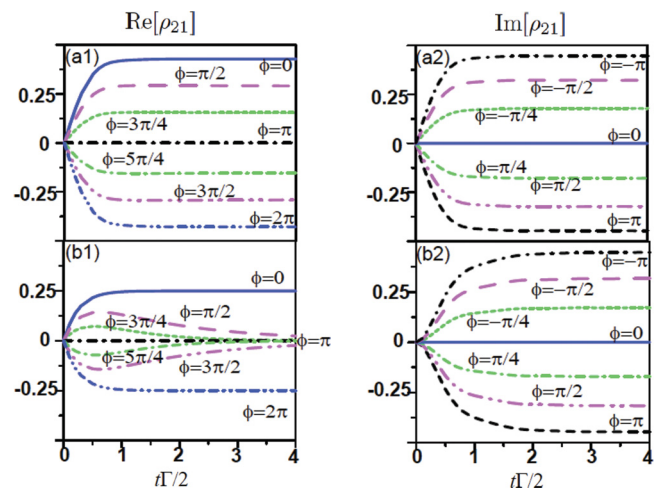


FIG. 4. (Color online) The full coherence time evolutions of ρ_{21} , (a1) and (a2), in the large asymmetrical coupling ($\delta\Gamma = 0.9\Gamma$), compared with the phase localization, (b1) and (b2), in the symmetrical couplings ($\delta\Gamma = 0$), the letter was shown in our previous work (Ref. 33), as well as in Ref. 35.

intrinsic property of this pseudospin system, independent of the coupling geometry and the bias configurations. Besides, we can calculate the tunneling current to reservoir $\alpha = L, R$ within the same framework:²⁶ $I_\alpha(t) = e \sum_i \text{tr}_s[\mathcal{L}_{i\alpha}^+(t)\rho(t)]$. The steady-state transport current $I = \frac{1}{2}(I_L - I_R)$ has been calculated³²

$$I(\phi) = \int \frac{d\omega}{2\pi} [f_L(\omega) - f_R(\omega)] \mathcal{T}(\omega, \phi), \quad (11)$$

where the transmission coefficient is given by

$$\mathcal{T}(\omega, \phi) = \frac{(\Gamma^2 - \delta\Gamma^2) [\omega^2 \cos^2 \frac{\phi}{2} + \frac{1}{4} \delta E \sin^2 \frac{\phi}{2}]}{[\omega^2 + \Gamma_+^2(\phi)][\omega^2 + \Gamma_-^2(\phi)]}. \quad (12)$$

By taking $\delta\Gamma = 0$ it reproduces the result of the authors of Ref. 28. Equation (12) clearly shows that the transport current has a period in the AB flux of 2π . This 2π period, as a feature for the coherence of transport, is well known and has been observed in experiments.^{16,22,23} The 4π period, a nontrivial character of the quantum state of the DQD molecule, requires further experimental investigation. Note that although the coherent phase of the off-diagonal density matrix element is gauge dependent, the AB flux dependence of the coherence phase and its periodicity are both independent of the gauge choice.

In summary, we have demonstrated the unusual conditions for the coherence control of DQD artificial molecules using AB fluxes. We have analyzed the AB flux-dependent coherence controlling through the exact solution of the master equation.

When a large bias is applied with a strong asymmetry in couplings to the source and the drain, coherent control by the AB flux can be achieved. The decoherence induced by the electron tunnelings can be efficiently suppressed. We also find that the period of the quantum state of the DQD molecule in the AB flux is 4π , in contrast with the 2π periodicity of the transport current. The revelation of the underlying quantum coherence of the molecular states is thus beyond the usual transport measurement. The verifications of these molecular states would rely on a suitable quantum-state-tomography protocol for further investigations. We hope that this theory for DQD molecules could inspire new experiments on coherence control of molecular states via AB fluxes, and become also useful for the quantum emulation³⁸ of artificial molecular processes.

ACKNOWLEDGMENTS

M.W.Y.T. and W.M.Z. are supported partially by the National Science Council of ROC under Contract No. NSC-99-2112-M-006-008-MY3, and F.N. is partially supported by the ARO, NSF Grant No. 0726909, JSPS-RFBR Contract No. 12-02-92100, Grant-in-Aid for Scientific Research (S), MEXT Kakenhi on Quantum Cybernetics, and the JSPS via its FIRST program. M.W.Y.T. and W.M.Z. also acknowledge the support of the computing facility from the HPC Center of the National Cheng Kung university and the National Center for Theoretical Science. We also thank Michihisa Yamamoto for useful discussions.

*wzhang@mail.ncku.edu.tw

†fnori@riken.jp

- ¹J. Q. You and F. Nori, *Nature* **474**, 590 (2011); *Phys. Today* **58**, 42 (2005).
- ²R. Hanson, L. P. Kouwenhoven, J. R. Petta, S. Tarucha, and L. M. K. Vandersypen, *Rev. Mod. Phys.* **79**, 1217 (2007).
- ³I. Buluta, S. Ashhab, and F. Nori, *Rep. Prog. Phys.* **74**, 104401 (2011).
- ⁴J. J. L. Morton, D. R. McCamey, M. A. Eriksson, and S. A. Lyon, *Nature (London)* **479**, 345 (2011).
- ⁵D. Loss and D. P. DiVincenzo, *Phys. Rev. A* **57**, 120 (1998).
- ⁶R. H. Blick and H. Lorenz, in *Proceedings of the IEEE International Symposium on Circuits and Systems*, edited by J. Calder, Vol. II (IEEE, Piscataway, NJ, 2000), p. 245.
- ⁷A. W. Holleitner, R. H. Blick, A. K. Huttel, K. Eberl, and J. P. Kotthaus, *Science* **297**, 70 (2002).
- ⁸T. Hatano, M. Stopa, and S. Tarucha, *Science* **309**, 268 (2005).
- ⁹T. Hayashi, T. Fujisawa, H. D. Cheong, Y. H. Jeong, and Y. Hirayama, *Phys. Rev. Lett.* **91**, 226804 (2003).
- ¹⁰J. Gorman, D. G. Hasko, and D. A. Williams, *Phys. Rev. Lett.* **95**, 090502 (2005).
- ¹¹J. R. Petta, A. C. Johnson, J. M. Taylor, E. A. Laird, A. Yacoby, M. D. Lukin, C. M. Marcus, M. P. Hanson, and A. C. Gossard, *Science* **309**, 1280 (2005).
- ¹²K. D. Petersson, J. R. Petta, H. Lu, and A. C. Gossard, *Phys. Rev. Lett.* **105**, 246804 (2010).

- ¹³Y. M. Galperin, B. L. Altshuler, J. Bergli, and D. V. Shantsev, *Phys. Rev. Lett.* **96**, 097009 (2006).
- ¹⁴I. V. Yurkevich, J. Baldwin, I. V. Lerner, and B. L. Altshuler, *Phys. Rev. B* **81**, 121305 (2010).
- ¹⁵D. C. B. Valente, E. R. Mucciolo, and F. K. Wilhelm, *Phys. Rev. B* **82**, 125302 (2010).
- ¹⁶A. Yacoby, M. Heiblum, D. Mahalu, and H. Shtrikman, *Phys. Rev. Lett.* **74**, 4047 (1995).
- ¹⁷D. Loss and E. V. Sukhorukov, *Phys. Rev. Lett.* **84**, 1035 (2000).
- ¹⁸K. Kang and S. Y. Cho, *J. Phys.: Condens. Matter* **16**, 117 (2004).
- ¹⁹T. Kubo, Y. Tokura, T. Hatano, and S. Tarucha, *Phys. Rev. B* **74**, 205310 (2006).
- ²⁰T. Hatano, T. Kubo, Y. Tokura, S. Amaha, S. Teraoka, and S. Tarucha, *Phys. Rev. Lett.* **106**, 076801 (2011).
- ²¹M. Yamamoto, S. Takada, C. Bauerle, K. Watanabe, A. D. Wieck, and S. Tarucha, *Nat. Nanotech.* **7**, 247 (2012).
- ²²A. W. Holleitner, C. R. Decker, H. Qin, K. Eberl, and R. H. Blick, *Phys. Rev. Lett.* **87**, 256802 (2001).
- ²³M. Sigrist, T. Ihn, K. Ensslin, D. Loss, M. Reinwald, and W. Wegscheider, *Phys. Rev. Lett.* **96**, 036804 (2006).
- ²⁴S. A. Gurvitz and Ya. S. Prager, *Phys. Rev. B* **53**, 15932 (1996); S. A. Gurvitz, *ibid.* **57**, 6602 (1998).
- ²⁵T. Fujisawa, T. Hayashi, and Y. Hirayama, *J. Vac. Sci. Technol. B* **22**, 2035 (2004).
- ²⁶M. W. Y. Tu and W. M. Zhang, *Phys. Rev. B* **78**, 235311 (2008); J. S. Jin, M. W. Y. Tu, W. M. Zhang, and Y. J. Yan, *New J. Phys.* **12**, 083013 (2010).

- ²⁷J. König and Y. Gefen, *Phys. Rev. Lett.* **86**, 3855 (2001).
- ²⁸B. Kubala and J. König, *Phys. Rev. B* **65**, 245301 (2002).
- ²⁹Z. T. Jiang, Q. F. Sun, X. C. Xie, and Y. Wang, *Phys. Rev. Lett.* **93**, 076802 (2004).
- ³⁰F. Li, X. Q. Li, W. M. Zhang, and S. A. Gurvitz, *Europhys. Lett.* **88**, 37001 (2009).
- ³¹V. I. Puller and Y. Meir, *Phys. Rev. Lett.* **104**, 256801 (2010).
- ³²Matisse Wei-Yuan Tu, W. M. Zhang, J. Jin, O. Entin-Wohlman, and A. Aharony, *Phys. Rev. B* **86**, 115453 (2012).
- ³³Matisse Wei-Yuan Tu, W. M. Zhang, and J. Jin, *Phys. Rev. B* **83**, 115318 (2011).
- ³⁴J. Schwinger, *J. Math. Phys.* **2**, 407 (1961); L. V. Keldysh, *Sov. Phys. JETP* **20**, 1018 (1965).
- ³⁵S. Bedkihal and D. Segal, *Phys. Rev. B* **85**, 155324 (2012).
- ³⁶When $\phi = 0$, the amplitude enhancement of the coherence is determined by the sign of $\delta\Gamma$. When $\mu_L > \mu_R$, the asymmetry of $\Gamma_L > \Gamma_R$ is preferred for larger ρ_{21} .
- ³⁷H. N. Xiong, W. M. Zhang, Matisse Wei-Yuan Tu, and D. Braun, *Phys. Rev. A* **86**, 032107 (2012).
- ³⁸I. Buluta and F. Nori, *Science* **326**, 108 (2009).